A Quadratic Conduction Gas Lens

By C. A. FRITSCH and D. J. PRAGER

(Manuscript received January 17, 1969)

A lens system for a periodic light-beam waveguide is proposed and analyzed in which gas is enclosed in a circular cylinder heated with a cos 2ϕ temperature distribution. We show that this temperature distribution may be produced by cutting a cylindrical hole in the center of a square block which has two opposite sides of equal temperature above the ambient temperature, and two sides of a lower temperature. Heat conduction across the gas produces an index of refraction variation which, in two orthogonal azimuthal planes, increases or decreases as the radius squared. The effect of thermal convection is analyzed by solving the governing equations as an expansion in powers of the Rayleigh number; the solution reveals that convection effects can be made negligible over a practical range of lens parameters. The major attributes of the lens system are that only temperature controls are required and the aberrations associated with thermal convection can be readily minimized.

I. INTRODUCTION

A gas lens system to transmit a light beam through a tube should have a favorable refractive index, negligible aberrations, and a simple construction. The favorable refractive index must be such that all light rays parallel to the tube axis, but of varying distances from that axis, converge at approximately the same point on the axis, the distance being called the focal length. Within the paraxial ray approximation it is easy to show that an r^2 variation of the refractive index has this property (see, for example, Refs. 1 and 2).

Berreman obtained a refractive index (which varied approximately as the square of the radius) by flowing a gas through a cold cylinder enclosing a warm helix aligned on the axis.[3] The interior of the helix has the desired refractive index. Marcuse and Miller simplified Berreman's lens by considering a cool gas flowing through a heated cylinder of uniform temperature (the Graetz problem).[1,2]

In order to reduce the distortion resulting from spherical aberrations, Berreman built a counterflow arrangement composed of two back to back tubular lenses.[4] Marcuse calculated the principal surfaces of a flow type lens noting that the one with the light beam parallel to the flow differs only slightly from that of the beam antiparallel to the flow.[2] He then numerically calculated the fate of a beam as it passes through a large number of flow lenses and compared the results with those with a counterflow arrangement.[5] This arrangement decreased the distortion. Kaiser later found that this configuration also lessens the asymmetric distortion due to thermal convection.[6]

The major drawback to the flow-type lens is the need for control of the flow. Gu performed a compressible flow analysis and found that, as a result of the wall friction, choking could occur for the optimal flow rate in a few hundred meters.[7] This could be overcome only by further complexities in the system.

A conduction-type lens was proposed by Suematsu, Iga, and Ito, in which they analyzed a configuration composed of hyperbolic, convex inward walls, two of which are at one temperature and the other opposing two at a lower temperature.[8] The concomitant temperature distribution varies as the square of the distance in the transverse direction. Then the refractive index bears the r^2 variation* in two orthogonal planes, being convergent in one and divergent in the other. This guadratic variation has two highly desirable characteristics. First, within the paraxial approximation, the focal length of every ray passing through a quadratic lens is independent of the radius, and hence the field reproduces itself after each period.[1] Second, Marcatili has shown that the eigenfunctions associated with a quadratic lens are Gaussian. Therefore a laser beam which is also Gaussian can be mode-matched to a waveguide consisting of quadratic lenses. This means that all the energy will remain in the launched mode; the only mode conversion that would take place is that resulting from higher order variation, that is, aberrations.

The advantage of the conduction lens is that only temperature controls are required since no gas flow is involved. However, thermal convection is present in this lens and although Suematsu, and others, observed a degradation of their lens at high temperature differences they did not analyze the thermal convection effects.

---

* For negligible pressure changes the refractive index is virtually only a function of the temperature; for small temperature variations the changes in refractive index are directly proportional to and of opposite sign from the temperature changes.

We will consider a quadratic conduction-type lens, which is formed by imposing a cos 2ϕ temperature distribution on the wall of a circular cylinder. For sufficiently small temperature variations the change in the refractive index is approximately quadratic and lensing action similar to that of Suematsu, and others, is obtained. The three central questions considered are: (*i*) What are the effects of thermal convection on the quadratic distribution? (*ii*) How does one readily obtain a cos 2ϕ wall temperature distribution? (*iii*) What are the optical properties of a waveguide consisting of these lenses?

We show that the cos 2ϕ distribution can be achieved very simply by boring a circular hole in a square block in which two opposite sides bear a higher temperature than ambient and the other two bear a lower temperature. If sections of the above lens are placed in tandem, each consecutive one rotated by 90 degrees, there then exists in one plane a series of alternating, convergent-divergent lenses. In the perpendicular plane this series is, so to speak, 180 degrees out of phase. We may then use Miller's[9] analysis of a sequence of alternating gradient lenses,* and determine criteria for the optical properties as a function of the parameters of the system.

We study the effect of thermal convection by using a straightforward perturbation analysis which is found to be in agreement with preliminary results of an experiment. We investigate the method of producing the wall temperature distribution by constructing an approximate solution which reveals how the wall temperature distribution can be established, as well as discuss the experimental program in progress and compare this lens and the other cited above.

II. ANALYSIS

2.1 *Analysis of Thermal Convection*

Consider a circular cylinder with the geometry given in Fig. 1. The governing equations for the steady motion of the gas within the cylinder are:

(*i*) continuity equation,

$$\nabla \cdot (\rho \mathbf{u}) = 0; \tag{1}$$

(*ii*) equation of motion,

$$\rho(\mathbf{u} \cdot \nabla)\mathbf{u} + \nabla p - \rho \mathbf{g} - \mu \nabla^2 \mathbf{u} = 0; \tag{2}$$

* Alternating gradient focusing in gas lens systems was first proposed by A. R. Hutson.[3]

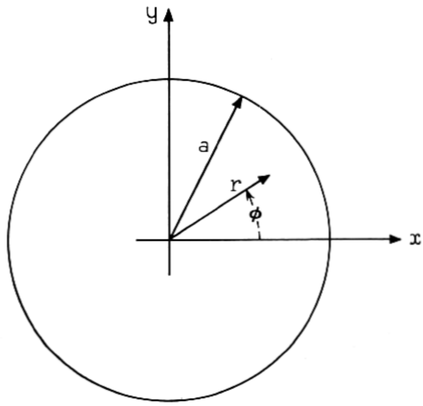

Fig. 1 — Geometry of the lens cylinder.

(*iii*) energy equation,

$$\rho \mathbf{u} \cdot \nabla (c_p T) = k \nabla^2 T + \mathbf{u} \cdot \nabla p + \mu \Phi. \tag{3}$$

Here,

ρ is the density,
$\mathbf{u}$ the velocity,
p the pressure,
$\mathbf{g}$ the gravitational acceleration,
μ the viscosity,
c_p the specific heat at constant pressure,
k the thermal conductivity, and
Φ the dissipation function (associated with the frictional work).

The boundary conditions at the cylinder surface are

$$T(a, \phi) = T_o\left(1 + \frac{\Delta T}{T_o} \cos 2\phi\right) \tag{4}$$

and

$$\mathbf{u}(a, \phi) = 0, \tag{5}$$

where ΔT is the maximum excursion about the average wall temperature, T_o.

At this point we use the Boussinesq approximation which consists of two elements; the density changes are significant only in the body force term, and these changes are a function of temperature only. The latter element amounts to neglecting the product of the isothermal compressibility, κ, times the pressure change in comparison with the product of the volumetric expansivity, β, times the temperature change. In other words, for $\rho = \rho(p, T)$

$$\frac{d\rho}{\rho} = \frac{1}{\rho}\left(\frac{\partial\rho}{\partial p}\right)_T dp + \frac{1}{\rho}\left(\frac{\partial\rho}{\partial T}\right)_p dT$$

$$= \kappa\, dp - \beta\, dT,$$

and the Boussinesq approximation requires the second term to be much larger than the first term but still small enough so that

$$\rho = \rho_0[1 - \beta(T - T_o)], \tag{6}$$

where the subscript denotes conditions at the center of the cylinder in the absence of fluid motion.

We nondimensionalize the variables in the hope that a perturbation scheme for a solution to our problem may be suggested. We define

$$\mathbf{U} = \frac{\mathbf{u}}{k/(\rho_o c_p a)}, \qquad \mathbf{x} = \mathbf{X}/a, \qquad \theta = \frac{T - T_o}{\Delta T}. \tag{7}$$

Since the density changes are considered important only in the body force term, equation (1) yields the incompressible continuity equation,

$$\nabla \cdot \mathbf{U} = 0. \tag{8}$$

The pressure term can be eliminated from the equation of motion by taking the curl of equation (2). The result of this operation leads us to define the velocity components in terms of the stream function ψ so that in cylindrical coordinates we have

$$U_r = \frac{1}{r}\frac{\partial\psi}{\partial\phi}, \qquad U_\phi = -\frac{\partial\psi}{\partial r}. \tag{9}$$

The continuity equation, (8), is identically satisfied, and the equation of motion becomes

$$\sigma\nabla^4\psi + \frac{1}{r}\left(\frac{\partial\psi}{\partial r}\frac{\partial}{\partial\phi} - \frac{\partial\psi}{\partial\phi}\frac{\partial}{\partial r}\right)\nabla^2\psi = \sigma\lambda\left(\cos\psi\frac{\partial}{\partial r} - \frac{\sin\phi}{r}\frac{\partial}{\partial\psi}\right)\theta, \tag{10}$$

where

$$\sigma = \frac{\mu c_p}{k}, \quad \text{the Prandtl number, and}$$

$$\lambda = \frac{\beta\,\Delta T g c_p \rho_0^2 a^3}{\mu k}, \quad \text{the Rayleigh number.}$$

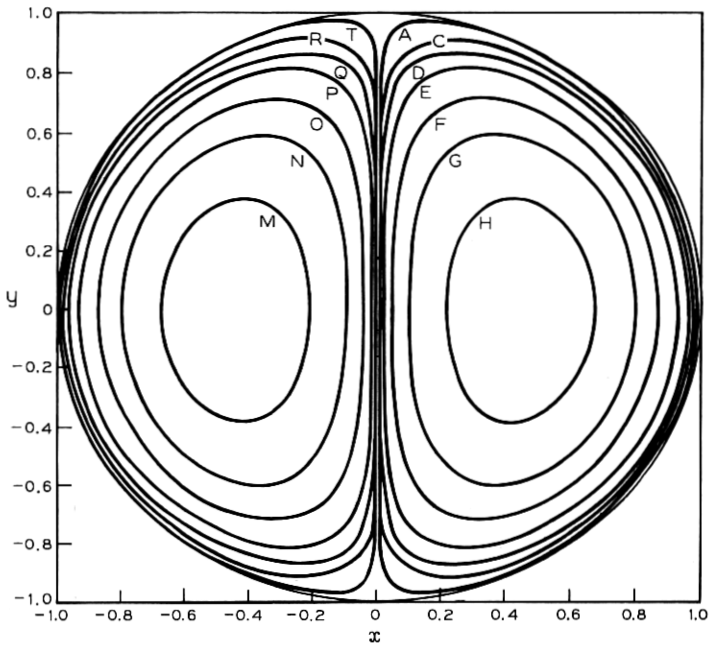

Fig. 2 — Contour plot of the first approximation for the stream function with values of $\psi^{(1)}$ on indicated contours:

A = 0.00001	F = 0.0005	M = −0.002	Q = −0.0001
C = 0.00005	G = 0.001	N = −0.001	R = −0.00005
D = 0.0001	H = 0.002	O = −0.0005	T = −0.00001
E = 0.0002		P = −0.0002	

If the velocities are sufficiently small then the viscous dissipation can be neglected and the energy equation, (3), in terms of the new variable becomes

$$\nabla^2\theta - \frac{1}{r}\left(\frac{\partial\psi}{\partial r}\frac{\partial}{\partial\phi} - \frac{\partial\psi}{\partial\phi}\frac{\partial}{\partial r}\right)\theta = 0. \tag{11}$$

The boundary conditions, (4) and (5), become

$$\theta(1, \phi) = \cos 2\phi \tag{12}$$

and

$$\frac{\partial\psi}{\partial r}(1, \phi) = \frac{\partial\psi}{\partial\phi}(1, \phi) = 0. \tag{13}$$

In the case of a small Rayleigh number it is fruitful to seek a solution in powers of λ;

$$\psi = \lambda\psi^{(1)} + \lambda^2\psi^{(2)} + \cdots \tag{14}$$

and

$$\theta = \theta^{(0)} + \lambda\theta^{(1)} + \lambda^2\theta^{(2)} + \cdots . \tag{15}$$

This expansion is valid in the limit, $\lambda \to 0$, and an upper bound of λ for the validity of the expansion will be obtained subsequently.

When we insert equations (14) and (15) into (10) and (11), the coefficients of like powers of λ must individually be set equal to zero for the equations to hold as λ is varied. Beginning with the lowest order we obtain from equation (11)

$$\nabla^2\theta^{(0)} = 0. \tag{16}$$

The solution to the equation, with the boundary condition given by equation (12), is

$$\theta^{(0)}(r, \phi) = r^2 \cos 2\phi. \tag{17}$$

Next, from equation (10) the lowest order contribution to the stream function is obtained from

$$\nabla^4\psi^{(1)} = \cos\phi \frac{\partial\theta^{(0)}}{\partial r} - \frac{\sin\phi}{r}\frac{\partial\theta^{(0)}}{\partial\phi} \tag{18}$$

with the boundary conditions given by equation (13). Inserting equation (17) into equation (18) and expressing the biharmonic operator in cylindrical coordinates yield

$$\left(\frac{\partial^4}{\partial r^4} + \frac{2}{r}\frac{\partial^3}{\partial r^3} - \frac{1}{r^2}\frac{\partial^2}{\partial r^2} + \frac{1}{r^3}\frac{\partial}{\partial r} - \frac{2}{r^3}\frac{\partial^3}{\partial\phi^2\,\partial r} + \frac{2}{r^2}\frac{\partial^4}{\partial\phi^2\,\partial r^2} + \frac{1}{r^4}\frac{\partial^4}{\partial\phi^4} + \frac{4}{r^4}\frac{\partial^2}{\partial\phi^2}\right)\psi^{(1)} = 2r\cos\phi. \tag{19}$$

The solution to this inhomogeneous biharmonic equation is

$$\psi^{(1)}(r, \phi) = \frac{1}{96}[r^4 - 2r^2 + 1]r\cos\phi. \tag{20}$$

Figure 2 is a contour plot of the stream function, equation (20).

Finally we wish to determine the perturbation on $\theta^{(0)}$. This will indicate the effect of thermal convection in distorting the lens and afford an estimation of the upper bound of the Rayleigh number. Again, from equation (11) we get

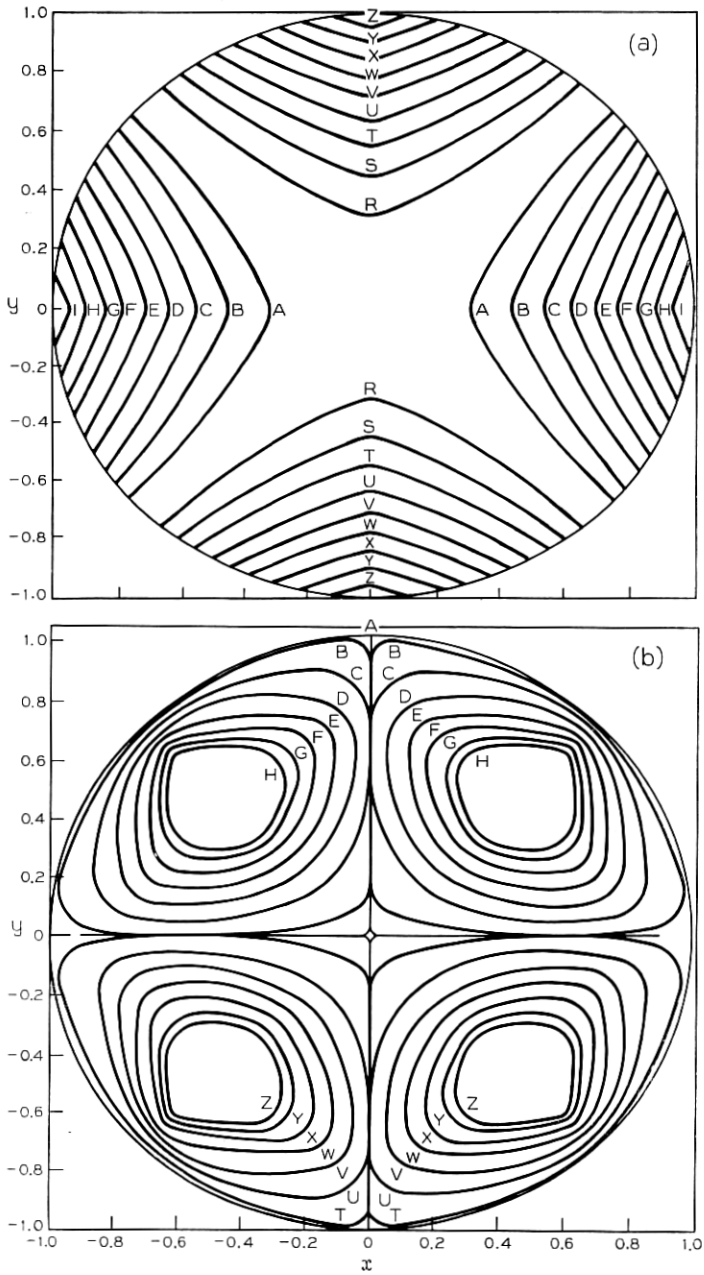
(a)
(b)
A B C D E F G H I
R S T U V W X Y Z
y
x
1.0
0.8
0.6
0.4
0.2
0
−0.2
−0.4
−0.6
−0.8
−1.0

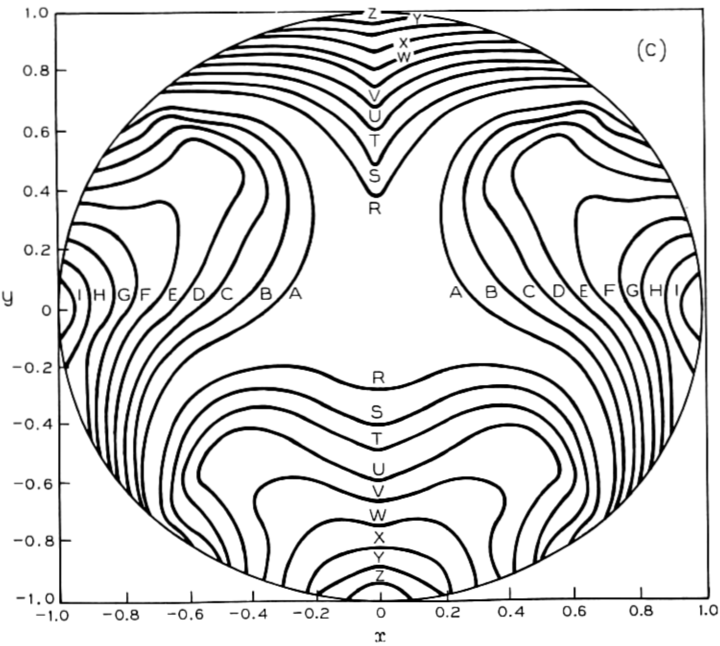

Fig. 3 — Contour plot of the (a) zeroth approximation for the temperature distribution with values of $\theta^{(0)}$ on indicated contours:

A = 0.1 = −R	D = 0.4 = −U	G = 0.7 = −X
B = 0.2 = −S	E = 0.5 = −V	H = 0.8 = −Y
C = 0.3 = −T	F = 0.6 = −W	I = 0.9 = −Z

(b) first perturbation for the temperature distribution with values of $\theta^{(1)}$ on indicated contours:

A = 0.0001 = −S	C = 0.005 = −U	E = 0.015 = −W	G = 0.025 = −Y
B = 0.001 = −T	D = 0.01 = −V	F = 0.02 = −X	H = 0.028 = −Z

(c) first approximation for the temperature distribution ($\lambda = 10^3$) with values of $\theta^{(0)} + \lambda\theta^{(1)}$ on indicated contours:

A = 0.1 = −R	D = 0.4 = −U	G = 0.7 = −X
B = 0.2 = −S	E = 0.5 = −V	H = 0.8 = −Y
C = 0.3 = −T	F = 0.6 = −W	I = 0.9 = −Z

$$\nabla^2\theta^{(1)} = \frac{1}{r}\left(\frac{\partial\psi^{(1)}}{\partial\phi}\frac{\partial\theta^{(0)}}{\partial r} - \frac{\partial\psi^{(1)}}{\partial r}\frac{\partial\theta^{(0)}}{\partial\phi}\right) \tag{21}$$

with the boundary condition

$$\theta^{(1)}(1, \phi) = 0. \tag{22}$$

Inserting equation (17) and (10) into equation (21) yields

$$\left(\frac{\partial^2}{\partial r^2} + \frac{1}{r}\frac{\partial}{\partial r} + \frac{1}{2}\frac{\partial^2}{\partial \phi^2}\right)\theta^{(1)} = -2(r^4 - 2r^2 + 1)r \sin\phi \cos 2\phi$$

$$+ 2(5r^4 - 6r^2 + 1)r \cos\phi \sin 2\phi. \qquad (23)$$

The solution which satisfies equation (22) is

$$\theta^{(1)}(r, \phi) = [f_1(1) - f_2(1)]\frac{r}{2}\sin\phi - [f_1(1) + f_2(1)]\frac{r^3}{2}\sin 3\phi$$

$$+ f_1(r)\sin\phi\cos 2\phi + f_2(r)\cos\phi\sin 2\phi, \qquad (24)$$

where

$$f_1(r) \equiv \frac{r^4}{96}\left(\frac{32}{379} - \frac{48}{2041}r^2\right)$$

and

$$f_2(r) \equiv \frac{r^3}{4(96)}\left(2r^4 - \frac{48(31)}{2041}r^3 - 4r^2 + \frac{32(11)}{379}r + 2\right).$$

A numerical calculation reveals that the maximum value of $\theta^{(1)}$ is approximately 3×10^{-4}. Since $\theta^{(0)}$ is bounded by unity, the expansion should be valid for Rayleigh numbers less than the order of 10^4. Figures 3a, b, and c show contour plots of $\theta^{(0)}$, $\theta^{(1)}$, and $\theta^{(0)} + \lambda\theta^{(1)}$, respectively. In Fig. 3c, $\lambda = 10^3$ to demonstrate the distortion possible.

Experiments are being conducted to verify the foregoing results and to better understand thermal convection in other circumstances. Figure 4 is a photograph of the streamlines made visible by the introduction of cigarette smoke into a circular cylinder having a cos 2ϕ temperature distribution. The Rayleigh number is 575. Notice the resemblance between this pattern and the contour plot of the preceding analytical results (Fig. 2). The slight shift upward of the smoke streamlines can be attributed to higher order terms in θ and ψ. The steadiness of the observed flow supports our seeking time-independent solutions of the equations of motion.

2.2 *Establishing the cos 2ϕ Wall Temperature Distribution*

If one imposes a linear temperature distribution across a slab by heating one face and cooling the other, and then if one drills a cylindrical hole parallel to the faces of the slab, it is well known that a temperature distribution varying as cos ϕ will appear on the wall of the cylindrical hole. Extending this to a square region with one pair of opposite faces heated and the other pair cooled one might presume that a cos 2ϕ temperature distribution would appear on a cylindrical hole cut in the center of the square. To determine the degree of approximation of this presumption the heat conduction problem in a region bounded on the exterior by a square and on the interior by a circle is analyzed in the following paragraphs. Figure 5 shows the geometry of the problem.

The problem of a square with a hole in it cannot be solved exactly, as we show. An approximate solution could be sought in either cartesian or cylindrical coordinates. However, considering the problem in cylindrical coordinates allows one to compare the relative magnitude of the portion of the distribution, which varies with cos 2ϕ, to that associated with higher order terms. Secondly, the solution is more nearly

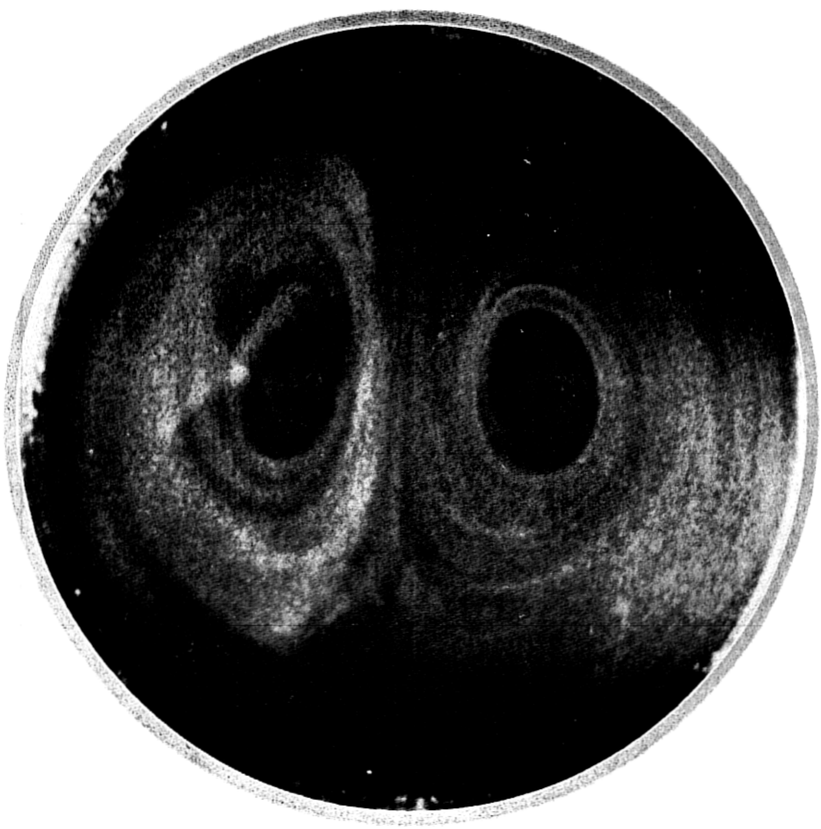

Fig. 4 — Convective motion illuminated by cigarette smoke.

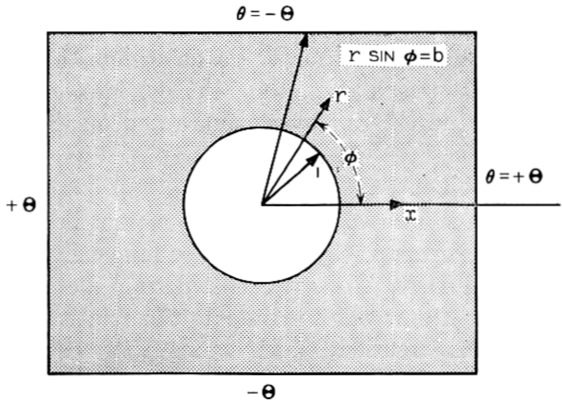

Fig. 5 — Geometry for conduction problem in solid cross section of gas lens.

exact on the cylindrical hole if the approximate solution is sought in cylindrical coordinates. Furthermore, since the heating arrangement has a certain amount of symmetry, only a sector $\pi/4 \leqq \phi \leqq \pi/2$ need be considered.

For steady two-dimensional conduction in a material having constant thermal conductivity the heat conduction equation becomes

$$\frac{\partial^2 \theta}{\partial r^2} + \frac{1}{r}\frac{\partial \theta}{\partial r} + \frac{1}{r^2}\frac{\partial^2 \theta}{\partial \phi^2} = 0. \tag{25}$$

The boundary conditions are:

$$\text{at} \quad r \sin \phi = b, \qquad \theta = -\Theta; \tag{26}$$

$$\text{at} \quad r = 1, \qquad \frac{\partial \theta}{\partial r} = 0; \tag{27}$$

$$\text{at} \quad \phi = \frac{\pi}{4}, \qquad \theta = 0; \tag{28}$$

$$\text{at} \quad \phi = \frac{\pi}{2}, \qquad \frac{\partial \theta}{\partial \phi} = 0. \tag{29}$$

Notice that $\theta = (T - T_o)/\Delta T$ as before, where T is the temperature excursion desired on the cylindrical hole. Consequently, $\Theta = (T_w - T_o)/\Delta T$ where T_w is the wall temperature. The insulated condition, (27), assumes that the heat lost to the gas in the hole is negligibly small compared with the heat conduction in the solid. This is reasonable as long as $k_{solid} \gg k_{gas}$.* Condition (29) results from the symmetry about $\pi/2$. The radius r is normalized with respect to the cylinder radius as in the Section 2.1.

Assume a separable solution of the form

$$\theta = R(r)\Phi(\phi), \tag{30}$$

so that

$$r^2R'' + rR' - \alpha^2 R = 0, \tag{31}$$

$$\Phi'' + \alpha^2\Phi = 0. \tag{32}$$

The solution of equation (31) and (32) is

$$\theta = A\left(r^\alpha + \frac{B}{r^\alpha}\right)(C \sin \alpha\phi + \cos \alpha\phi). \tag{33}$$

The insulated condition (27) is satisfied if $B = 1$. To satisfy both conditions (28) and (29) simultaneously, $C = 0$ and

$$\alpha = 2n, \qquad n = 1, 3, 5, \cdots . \tag{34}$$

Therefore,

$$\theta_n = A_n\left(r^{2n} + \frac{1}{r^{2n}}\right)(\cos 2n\phi), \qquad n = 1, 3, 5, \cdots , \tag{35}$$

where A_n is determined to satisfy equation (26), that is,

$$-\Theta = \sum_{n=1,3,5,\cdots}^{\infty} A_n\left(\frac{b^{2n}}{\sin^{2n}\phi} + \sin^{2n}\phi\right) \cos 2n\phi. \tag{36}$$

Because of equation (26) our problem in r is not a Sturm-Liouville system and we have no assurance that equation (36) will converge even if the A_n's could be determined in general. In what follows we determine the first few A_n's so that equation (36) is satisfied in two different senses as accurately as our needs dictate—collocation and minimization of the error in a least-squares sense.[10]

In the collocation method the error is made to vanish at, say, three particular points on the boundary $r \sin \phi = b$. This gives us three simultaneous equations through which A_1, A_3, and A_5 can be determined. For two different sets of collocation points, the corresponding coefficients are listed in Table I for the ratio of the side length to the

* The k for most plastics is a factor of 10 greater than that for air. For formed plastics $k_{solid} \approx k_{gas}$ and the behavior of θ at $r = 1$ can be assessed from the solution for conduction in a square with two sides at Θ and two sides at $-\Theta$.

TABLE I—COEFFICIENTS FOR APPROXIMATE SOLUTION BY COLLOCATION

	Collocation points = 60°, 75°, and 90°		
	$b = 2$	$b = 4$	$b = 6$
a_1	1.03531	1.08889	1.09191
a_3	−0.11082	−0.10469	−0.10434
a_5	0.01083	0.01155	0.01159

	Collocation points = 50°, 70°, and 90°		
	$b = 2$	$b = 4$	$b = 6$
a_1	1.04521	1.09927	1.10232
a_3	−0.14096	−0.13457	−0.13421
a_5	0.03046	0.03101	0.03104

cylinder diameter, $b = 2, 4, 6$. These coefficients are normalized with respect to Θ. Furthermore, some of the dependence on b is suppressed when the coefficients are defined as:

$$a_n = \frac{A_n b^{2n}}{\Theta}, \tag{37}$$

so that

$$\frac{\theta}{\Theta} \cong \sum_{n=1,3,5} \frac{a_n}{b^{2n}} \left(r^{2n} + \frac{1}{r^{2n}} \right) \cos 2n\phi, \qquad \frac{\pi}{4} \leqq \phi \leqq \frac{\pi}{2}. \tag{38}$$

Figure 6 contains a plot of $\theta(r = b/\sin\phi, x/b)$ using both sets of collocation points. This illustrates the degree of approximation entailed at the outer boundary where $-(\theta/\Theta)$ should equal unity over $0 \leqq X/b < 1$.

The least-squares method requires that the mean square error over the boundary $r = b/\sin\phi$, $\pi/4 \leqq \phi \leqq \pi/2$, be as small as possible. Defining

$$\epsilon = \theta - (-\Theta); \tag{39}$$

we then wish to minimize

$$\int_{\pi}^{\pi} \epsilon^2 \, d\phi. \tag{40}$$

For convenience we take only the first two terms of equation (35) for θ and note that $r^{2n} \gg 1/r^{2n}$ close to the outer boundary so long as $b \geqq 2$. Consequently,

$$\theta \cong A_1 r^2 \cos 2\phi + A_3 \cos 6\phi, \tag{41a}$$

and

$$\epsilon \cong A_1 b^2 \frac{\cos 2\phi}{\sin^2 \phi} + A_3 b^6 \frac{\cos 6\phi}{\sin^6 \phi}. \tag{41b}$$

Inserting equation (41b) into integral (40), performing the integration, and setting the derivative with respect to A_1 and A_3 equal to zero we find that:

$$\frac{\theta}{\Theta} \cong \frac{1.3118}{b^2}\left(r^2 + \frac{1}{r^2}\right) \cos 2\phi - \frac{0.1805}{b^6}\left(r^6 + \frac{1}{r^6}\right) \cos 6\phi. \tag{42}$$

Figure 6 also has a plot of equation (42) evaluated at $r = b/\sin \phi$. Apparently the collocation method yields a much closer approximation for heat conduction problems. (The square of the temperature has no particular physical meaning.)

Returning to the collocation solution (Table I) the temperature distribution on the cylindrical wall, for $b = 6$, is given as

$$\frac{\theta(1, \phi; 6)}{\Theta} \cong \frac{2a_1 \cos 2\phi}{6^2} + \frac{2a_3 \cos 6\phi}{6^6} + \frac{2a_5 \cos 10\phi}{6^{10}}$$

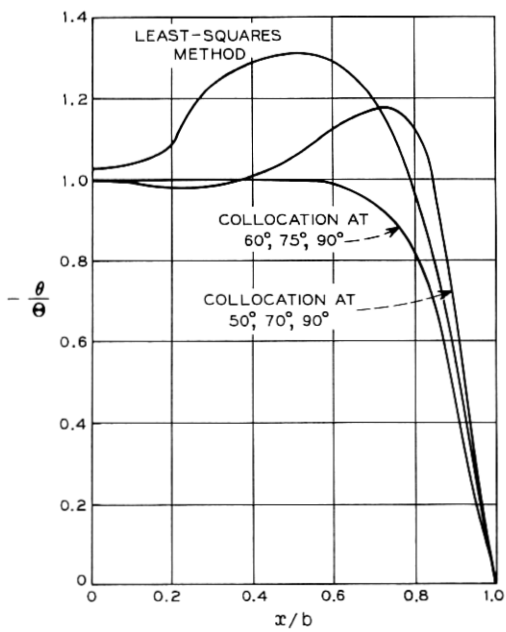

Fig. 6 — Comparison of approximation at outer boundary in conduction problem.

$$\cong 0.06066 \cos 2\phi - 0.0447 \times 10^{-4} \cos 6\phi + 0.0383 \times 10^{-8} \cos 10\phi, \tag{43}$$

and we see that the distribution varies as cos 2ϕ within one part in 10,000. For $b = 2$ the deviation is somewhat greater, being

$$\frac{\theta(1, \phi; 2)}{\Theta} = 0.5176 \cos 2\phi - 0.00346 \cos 6\phi + 0.02115 \times 10^{-3} \cos 10\phi. \tag{44}$$

Similar results can be obtained from equation (42).

Recall that this solution is for $k_{\text{solid}} \gg k_{\text{gas}}$. When $k_{\text{solid}} \approx k_{\text{gas}}$ the deviation of $\theta(1)$ from cos 2ϕ can be evaluated from the analytical solution for a solid square two sides at Θ and two other sides at $-\Theta$, *v.*[11] In doing this we found that the deviations from cos 2ϕ are of the same order as those cited above.

The power necessary to operate the lens can be readily found from integrating along the radial line at $\phi = \pi/4$. The heat flow rate $\dot{Q}$ through one sector is given by

$$\dot{Q} = -k\,\Delta T \int_1^b \frac{1}{r} \frac{\partial \theta}{\partial \phi}\, dr$$

$$\dot{Q} = \Delta T \sum_{n=1,3,5} k A_n \sin \frac{n\pi}{2} \left[\left(\frac{2}{\sqrt{2}} \right)^{2n} - \frac{(\sqrt{2}/2)^{2n}}{b^{4n}} \right] \tag{45}$$

which is nearly independent of b. In terms of the collocation coefficients, where the b^{4n} term has been neglected,

$$\frac{\dot{Q}}{k\Theta\,\Delta T} \cong 2a_1 - 8a_3 + 32a_5 . \tag{46}$$

For $b = 4$

$$\dot{Q} = 3.38\, k\Theta\,\Delta T = 3.38\, k(T_w - T_o). \tag{47a}$$

Since

$$\theta(1, \pi/2; 4) = -0.136\Theta = -0.136\left(\frac{T_w - T_o}{\Delta T}\right) = 1, \tag{47b}$$

then for a ΔT of 1°C excursion $T_{\text{wall}} - T_o = 7.4°C$. For a gas lens whose solid portion is made of polystyrene ($k = 0.1$ W/m°C) the heat flow rate would be $Q = 2.5$ W/m for each sector; then the power requirement would be 10 W/m for 1°C ΔT across the lens. If a foamed polystyrene could be used the power requirement would be 3.5 W/m°C.

2.3 *Optical Properties of the Conduction Lens*

With the effect of thermal convection in mind we now consider how to evaluate the optical properties of a gas lens characterized by the lowest order temperature distribution (that is, $r^2 \cos 2\phi$). We wish to determine these properties as functions of ΔT, cylinder radius a, and lens section length L; we are constrained by the requirement of minimizing ΔT so that the distortion depicted in Fig. 3c shall be tolerable. In the following paragraphs we only write down the relevant equation; we do not establish explicit design criteria.

The system of lenses consists of a sequence of sections with each succeeding one rotated 90 degrees. Therefore, for any angle, ϕ (see Fig. 1), as one marches axially, the sections act alternately as divergent and convergent lenses. Since the temperature varies angularly, as well as radially, so does the refractive index; hence, in addition to the ray bending toward or away from the axis it will, in general, be twisted. However, at $\phi = 0$ and $\pi/2$ the refractive gradient has no angular gradient and, hence, rays originally in either of those planes remain there; they undergo convergent and divergent displacements alternately. All other rays have radial displacements intermediate to those at $\phi = 0, \pi/2$.

The trajectories of the rays in the $\phi = 0, \pi/2$ planes may be calculated analytically and turn out to be sinusoidal and exponential in the convergent and divergent sections, respectively.

Although a numerical solution must be used for the other trajectories, some qualitative observations may be made. In the neighborhood of $\phi = 0$ the angular component of the refractive index causes rays to be twisted away from that attitude, while near $\phi = \pi/2$ rays are restored to that angular position. Therefore, as one moves down a section the density of rays tends to increase near $\phi = \pi/2$ and to decrease near $\phi = 0$.

In order to obtain the intensity of the beam through a lens section, the Helmholtz-type equation with the appropriate refractive index must be solved. This was done by Marcatili[12] for an asymmetrical but convergent-type refractive index.* He established conditions for the stability of a lens system and calculated the focal length.

For our present purposes there is no need for a detailed solution of the field equations but rather for the ray displacement, stability criterion, and focal length. Toward this end Miller's[9] analysis of the

* Marcatili informed us that there is no basic reason why his analysis could not be extended to include divergent sections.

ray equation is applicable.† He obtained these quantities by solving the difference equations which govern the passage of the rays through the sequence of lenses. If we only consider the $\phi = 0, \pi/2$ planes, then the sections act as alternating convergent and divergent lenses, with the rays remaining in their original planes; we may then apply Miller's results.

Miller obtained the ray displacement after the nth convergent and mth divergent lens for an initially convergent and an initially divergent sequence. He also found the stability condition which keeps the ray trajectory bounded after an infinite number of lenses. This condition is

$$0 < \frac{L}{f} < 2. \tag{48}$$

Here, to serve as an example, we only display the expression for the ray displacement after the nth convergent lens for an initially convergent lens:

$$r_n = r_o k_1 \cos(n\,\delta - \phi_1) + r_0' L k_2 \sin n\,\delta \tag{49}$$

where r_o and r_o' are the initial displacement and slope, respectively, and

$$\delta = \cos^{-1}\left[1 - \frac{1}{2}\left(\frac{L}{f}\right)^2\right], \qquad k_1 = \frac{2}{1 - \dfrac{L}{2f}},$$
$$\phi_1 = |\cos^{-1} k_1^{-1}|, \quad \text{and} \quad k_2 = \frac{2 + \dfrac{L}{f}}{\sin \delta}. \tag{50}$$

Furthermore, we must stipulate that the ray does not intersect the cylinder wall, that is,

$$\frac{r_n}{a} < 1. \tag{51}$$

The relationship between the focal length and the refractive index may be obtained from Marcuse and Miller.[1] For a thin lens the focal length is given by*

† We are indebted to Marcatili for several clarifying remarks on this subject.
* A thin lens is one in which the principal surface generated by rays incident from the left coincides with that surface constructed by rays incident from the right. Since there is no preferred direction with the conduction-type lens it is thin; the flow-type lenses cited in Section I may be approximately thin.

$$f = \tfrac{1}{2}\beta_o \frac{r^2}{\Delta\phi}, \tag{52}$$

where $\beta_o = 2\pi/\lambda$, λ is the wave length of the light, and $\Delta\phi$ is the difference of the phase of a ray incident a distance r from and parallel to the axis after traveling a distance L, compared with a ray on the axis traveling the same distance.

To calculate $\Delta\phi$ in terms of the refractive index, we invoke the paraxial approximation in which the rays are regarded as approximately parallel to the axis. Then the required phases are easy to calculate, that is,

$$\phi(r, z) \cong \beta_o \int_0^L n(r)\, dx = \beta_o n(r) L \tag{53}$$

and

$$\phi(0, z) = \beta_o n(0) L. \tag{54}$$

The refractive index at $\phi = 0$ is

$$\begin{aligned} n(r, 0) &= 1 + (n_o - 1)\frac{T_o}{T(r, 0)} = 1 + \frac{n_o - 1}{1 + \dfrac{\Delta T}{T_o}\dfrac{r^2}{a^2}} \\ &\cong n_o - (n_o - 1)\frac{\Delta T}{T_o}\frac{r^2}{a^2}, \end{aligned} \tag{55}$$

where n_o is the refractive index at the axis at temperature T_o.

Hence,

$$\Delta\phi = \beta_o(n_o - 1)\frac{\Delta T}{T_o}\frac{r^2}{a^2} L \tag{56}$$

and the focal length is obtained from equation (52):

$$f = \frac{1}{2}\frac{a^2 T_o}{(n_o - 1)\,\Delta T L} \tag{57}$$

independent of r.

With the aid of equations (48), (49), (51), and (57) we may determine the focal length and ray displacement as a function of the lens section and radius and temperature excursion. For a complete discussion of the foregoing subject, see Ref. 9.

To establish precise design criteria the foregoing equations must be solved on a computer. However, for illustrative purposes and as one aspect of the problem we shall make use of some of Miller's simplified expressions valid in certain limits.[9]

If we use equation (49) with the value of the section length to focal length ratio which yields the smallest value of the maximum ray displacement and, furthermore, insure that the rays do not intersect the wall, ΔT obtained is unacceptable for three major reasons (*i*) the power requirement is excessive, (*ii*) the moderate Rayleigh number will cause appreciable distortion, and (*iii*) the temperature excursion is sufficiently large so that section end effects may be significant.

In order to overcome these objections we now examine the case of weak focusing, that is, $2f/L \gg 1$. We consider the initial conditions such that

$$r_o \ll r_o' f. \tag{58}$$

(The opposite inequality for weak focusing yields a trivial design problem since it does not involve the focal length.) From Miller the maximum ray radius, $r_{\max}$, is [9]

$$r_{\max} = 2 f r_0' . \tag{59}$$

To insure that the ray does not intersect the wall we have

$$\frac{a}{L} \geqq \frac{r_{\max}}{L}. \tag{60}$$

Inserting equations (57) and (59) into equation (60) yields

$$1 \geqq \frac{a}{L} \frac{T_o}{(n_o - 1)\,\Delta T} r_o' . \tag{61}$$

As an example we use the following values, where air is the medium of the lensing action

$$T_o = 290°\text{K},$$

$$n_o - 1 = 0.295 \times 10^{-3},$$

and

$$\lambda \text{ (Rayleigh number)} = 9.15 \times 10^7 \,\Delta T a^3$$

with ΔT in degrees Celsius and a in meters. In addition, let $r_0' = 10^{-4}$, $a = 3 \times 10^{-3}$m, and $L = 0.5$ m. Then from inequality (61) we obtain

$$\Delta T \geqq 0.59°\text{C}. \tag{62}$$

Hence, $\lambda = 2.9$. Consequently,

$$|\lambda\theta^{(1)}| < 10^{-3} \ll |\theta^{(0)}|_{max}\,.$$

It should be borne in mind that with the above values of a and L, the weak focusing limit is satisfied for $\Delta T \lesssim 5°C$. In addition, to satisfy inequality (58) with the foregoing values we must have

$$r_o \ll r_0'f = 1.5 \times 10^{-3}\ \text{m} \tag{63}$$

which is easy to satisfy.

Using equation (47a), we obtain for the heat flow rate through one sector

$$\dot{Q} = 1.5\ \text{W/m}$$

which results in a power requirement of 6.0 W/m. The required exterior wall temperature is calculated from equation (47b) as $T_w = T_o + 4.4°C$. Therefore, in the limit of weak focusing the temperature excursion is sufficiently small to make the lens system promising.

Considering the flow-type lens of Marcuse and Miller to have the same characteristics as the above conduction type lens, we calculate the power expended at optimum flow rate to be 1.14 W.[1] Hence, the lens proposed here requires somewhat more power for heating than those previously investigated. However, the flow-type lens also requires power to drive the gas.

Since the input beam will be more complicated then was assumed above, the foregoing calculation is very cursory. However, the reasonable magnitudes of a and L together with the small Rayleigh number lend encouragement to a more detailed analysis.

III. CONCLUSIONS AND RECOMMENDATIONS

The conduction-type lens proposed here is found to be feasible on the basis of negligible distortion resulting from thermal convection and reasonable power requirements to maintain the desired temperature distribution. Although the lens design illustrated was predicated on the weak focusing limit a wider range of parameters can be found by using Miller's complete expression.[9]

The effect of thermal convection was calculated from a two dimensional analysis, which is certainly valid away from the ends of the section since $a/L \ll 1$. For the temperature excursion required and the lens illustrated, the convection effect was found to be negligible. However, at the interface between the sections, the axial temperature gradients could be large depending on the spacing left between sections. Axial gradients were present in the experiments of Suematsu and others for their hyperbolic shaped conduction-type lens system.[8] They found that no significant aberration existed as long as $\Delta T < 42/a^{1.34}$ (a in millimeters) so that the effects of the axial gradients must have been insignificant.

The analyses presented indicate that a system of conduction-type lenses might be practical for an alternating gradient light-beam waveguide. Such a system would require straight square rods with a cylindrical hole. Two sides of the rod would be heated while the other two would be held at a uniform and constant temperature. This could be done by attaching aluminum fins which project into a constant temperature heat sink to the cooled sides. Such a heat sink is available for buried systems since, at depths greater than about five feet, the surface temperature changes are virtually damped out. Therefore, cooing is not required.

The hole in the rod would be of the order of 6 mm in diameter and the exterior could be as small as 2.4 cm across a face. Larger hole dimensions could be used but, for the same size beam and lensing action, the temperature difference and power requirement would increase proportionately.

After only a preliminary design analysis, where the simplest of Miller's expressions have been used, parameters have been obtained in the weak focusing limit which yield a power consumption somewhat greater than but of the same order of magnitude as flow-type gas lenses.[9] Additional investigations are, of course, necessary. The distortion of a gaussian beam as it is launched through a lens system should be numerically calculated (similar to Marcuse's study for the flow-type lens.[5]) The effect of the axial gradients that will be present at the interface between two lens sections will have to be assessed through experimental measurements of the optical performance of such a lens system.

REFERENCES

1. Marcuse, D., and Miller, S. E., "Analysis of a Tubular Gas Lens," B.S.T.J., *43,* No. 4 (July 1964), pp. 1759–1787.
2. Marcuse, D., "Theory of a Thermal Gradient Gas Lens," IEEE Trans., *MTT-13,* No. 6 (November 1965), pp. 734–739.
3. Berreman, D. W., "A Lens or Light Guide Using Convectively Distorted Thermal Gradients in Gases," B.S.T.J., *43,* No. 4 (July 1964), pp. 1469–1475.
4. Berreman, D. W., "Convective Gas Light Guides or Lens Trains for Optical Beam Transmission," J. Opt. Soc. Amer., *55,* No. 3 (March 1965), pp. 239–247.
5. Marcuse, D., "Deformation of Fields Propagating Through Gas Lenses," B.S.T.J., *45,* No. 8 (October 1966), pp. 1345–1358.

6. Kaiser, P., unpublished work.
7. Gu, A. L., unpublished work.
8. Suematsu, Y., Iga, K., and Ito, S., "A Light Beam Waveguide Using Hyperbolic-Type Gas Lenses," IEEE Trans., *MTT-14*, No. 12 (December 1966), pp. 657–667.
9. Miller, S. E., "Alternating-Gradient Focusing and Related Properties of Conventional Convergent Lens Focusing," B.S.T.J., *43*, No. 4 (July 1964), pp. 1741–1758.
10. Collatz, L., *The Numerical Treatment of Differential Equations,* New York: Springer-Verlag, 1966.
11. Carslaw, H. S., and Jaeger, J. C., *Conduction of Heat in Solids,* New York: Oxford University Press, 1959.
12. Marcatili, E. A. J., "Modes in a Sequence of Thick Astigmatic Lens-Like Focusers," B.S.T.J., *43,* No. 7 (Novemeber 1964), pp. 2887–2904.